Photocatalytic Reduction of Se(VI) in Aqueous Solutions in UV/TiO_2 System: Kinetic Modeling and Reaction Mechanism

Timothy T. Y. Tan, Donia Beydoun, and Rose Amal*

Centre for Particle and Catalyst Technologies, School of Chemical Engineering and Industrial Chemistry, University of New South Wales, Sydney, NSW 2052, Australia

Received: May 21, 2002; In Final Form: February 15, 2003

The kinetics of UV/TiO_2 photocatalytic reduction of Se(VI) in the presence of formic acid was investigated. Competitive adsorption models for the Se(VI) and $HCOO^-$ ions onto the same active sites on TiO_2 surface were derived, based on the adsorption of one Se(VI) ion onto two adsorptive sites. The use of the above adsorption models allows for the modeling of the Se(VI) photoreduction rates on the basis of the Langmuir−Hinshelwood (LH) reaction mechanism. The new model was able to represent the experimental data reasonably well, and it supported the experimental observation that the optimum Se(VI) photoreduction rate occurred at the molar adsorption ratio of formate-to-Se(VI) ions of approximately 3:1. A composite rate expression incorporating the effect of catalyst loading was also presented.

1. Introduction

Selenium (Se) and its compounds are widely used in industries for a variety of applications, such as production of glass, xerography, pesticides, photoelectric cells, and corrosion resistant stainless steel.[1] Se compounds have also been found in oil refinery wastewater and flushing water of fly ash from coal-fired power plants.[2] Se compounds have also been added as supplements in fertilizers to increase agricultural production.[3] Effluent from such industries and agricultural sources eventually produce selenium-laden wastewater. When present in low concentration, Se is an important trace nutrient for both humans and animals. Se deficiency has been shown to cause an increase in heart and liver disease and may be associated with an increased risk of cancer.[4] A dietary intake of about 50 μg/day for women and 70 μg/day for men is required for daily nutritional needs.[5] However, when consumed consistently at about 10 times the daily requirement, Se and its ions become toxic. Symptoms for Se toxicity include birth defects manifested in waterfowls,[6] skin disease, gastrointestinal disturbance, damage to the central nervous system, and death if taken in large doses.[7]

The dominant Se species in wastewater are selenate Se(VI) (SeO_4^{2-}), selenite Se(IV) (SeO_3^{2-}), and their protonated anions ($HSeO_4^-$ and $HSeO_3^{2-}$). Se can also exist in a variety of compounds, such as oxides/hydroxides, organoselenium compounds, and selenides.[8] However, Se(VI) ions are the species of environmental concern as they are more mobile due to minimal adsorption by soil particulates. Hence, most Se(VI) ions from industrial sources end up in waterways in the natural environment.[9,10] Physical,[11−14] chemical,[15−18] and biological[1,19−21] removal techniques have been employed and investigated to remove Se ions from wastewater. Physical removal techniques have shown little success in terms of Se(VI) removal. In addition, physical removal processes merely concentrate the Se compounds, rendering their subsequent disposal a major problem. Chemical removal techniques require long treatment times and involve a high chemical cost to achieve efficient removal of the selenium compounds, making them rather impractical in waste treatment. Biological removal techniques are highly sensitive to operating parameters, rendering such processes difficult to control.

Heterogeneous photocatalysis is an emerging technology that has been successfully applied in the degradation of toxic environmental pollutants.[22−35] This technology does not involve the addition of expensive and possibly harmful chemicals. It is also a sustainable technology that utilizes natural sunlight and recyclable catalyst. Its application in waste treatment is promising as some reviews involving pilot scale studies have already been undertaken to evaluate its economic viability.[36,37] Photocatalysis exploits the unique electronic structure of semiconductors to catalyze redox reactions. When exposed to ultraviolet or near UV-light, an electron (e^-) from the valence band (VB) is promoted to the conduction band (CB), simultaneously generating a hole (h^+) in the VB. This e^-−h^+ pair can recombine on the surface or in the bulk, or it can be captured by species adsorbed or close to the surface of the semiconductor.[32,38] An acceptor (A) capturing the e^- is hence reduced while a donor (D) reacting with the h^+ is oxidized, completing the redox cycle. Titanium dioxide (TiO_2) is the most widely investigated semiconductor photocatalyst due to its high stability, nontoxicity, and a redox potential that is capable of oxidizing a wide range of pollutants.[32]

Numerous works have been done to model heterogeneous photocatalytic reactions, based on the classical heterogeneous catalysis mechanism of Langmuir−Hinshelwood (LH) reaction mechanism. However, photocatalytic reactions are very complex and are affected by other operating parameters, such as catalyst dosage, light intensities, and temperature, of which the LH model could not fully predict. Some studies have proposed models for each operational parameter to elucidate their effects on the photocatalytic oxidation rate.[39−42]

Most of the published kinetic modeling studies have focused on the photooxidation of organic and inorganic pollutants that utilized dissolved oxygen gas as the electron acceptor.[43−47] Very little work on kinetic modeling has been done on the photoreduction of anionic toxic pollutants, such as chromate, nitrate,

* Corresponding author. Tel: 61-2-9385-4361. Fax: 61-2-9385-5966. E-mail: r.amal@unsw.edu.au.

10.1021/jp026149+ CCC: $25.00
Published on Web 04/10/2003

and selenate, which involves the simultaneous adsorption of the pollutant and organic scavenger. Gimenez et al.[48] proposed a model for catalyst deactivation in the photocatalytic reduction of chromate in the presence of oxygen. Alam and Montalvo[49] developed a kinetic model based on various electron and hole consuming reactions involving chromate as the anionic pollutant and salicylic acid and oxygen as the hole scavengers. Kikuchi and Sakamoto[50] proposed that, in the photocatalytic reduction of Se(VI) ions, when all the Se(VI) ions were reduced to elemental Se, no species in the solution could capture electrons from the conduction band of the TiO_2, while photogenerated holes continue to be captured by the organic reductant. This resulted in accumulated electrons in the conduction band, further reducing the elemental Se on the TiO_2 surface to hydrogen selenide (H_2Se). A model based on electron accumulation was proposed to explain their results.[50] Since H_2Se gas is toxic, it could be removed from the Se(VI) photoreduction system by passing the gas into Cu(II) solution, which acts to precipitate the selenide as CuSe.[51] CuSe is a useful p-type semiconductor.[52]

In our previous study,[53] it was found that the competitive adsorption of Se(VI) and formic acid (HCOOH) on the surface of TiO_2 played a significant role in optimizing the photocatalytic reduction of Se(VI). A molar adsorption ratio of 3:1 of formate: selenate was found to achieve optimum Se(VI) photoreduction rate. The present work follows on from those findings and aims to propose a kinetic model and a reaction mechanism by modeling the initial Se(VI) photoreduction rates in the presence of various HCOOH concentrations, based on the adsorption of both species. The proposed model will be used as the basis for optimization studies which will be carried out to verify the aforementioned ratio necessary to achieve optimum Se(VI) photoreduction rate.

2. Experimental Procedures

2.1. Catalyst and Reagent. Degussa P25 titanium dioxide was chosen as the photocatalyst. It is composed of approximately 70% anatase and 30% rutile, with a specific surface area of 49 m^2/g and approximately 25 nm as primary particles. The reagents used were all of analytical grade, and deionized pure water was used for the preparation of all solutions. Sodium selenate (Na_2Se0_4) was used to prepare Se(VI) solutions with concentrations of 0.256 and 0.512 mM (20 and 40 ppm). HCOOH (77 vol %) was used as the organic hole scavenger and its concentration was adjusted to the range of 1−25 mMC (15−300 ppmC). Copper(II) sulfate and sodium hydroxide were used to trap hydrogen selenide gas. The pH of the solution was maintained at pH 3.5 using sodium hydroxide and perchloric acid.

2.2. Experimental Apparatus and Procedure. The experimental setup has been previously described and illustrated.[53] It consists of a cylindrical glass reactor of 1.2 L capacity with a side quartz window through which UV was irradiated by a 200 W mercury lamp from the lamp housing (Oriel 66001-373). The photon flux into the reactor was determined to be 3.8 μmol photon/s by chemical actinometry.[54] Gas exhausted from the reactor was introduced into two traps in series, containing 5×10^{-3} M $CuSO_4$ and 0.1 M NaOH, respectively, to remove possible toxic hydrogen selenide gas (H_2Se) generated from the reduction process. The solution in the reactor was first purged with nitrogen (1.5 $dm^3\ min^{-1}$) and agitated by the magnetic stirrer for 30 min. The required amounts of Se(VI) and HCOOH were then added to make up a 1 L of test solution. This was followed by the adjustment of the pH to 3.5 using perchloric acid and then the addition titanium dioxide powder (0.5 gTiO_2/L). The pH was maintained at 3.5 throughout the reaction using perchloric acid and sodium hydroxide. The suspension was stirred for 30 min before being illuminated by the UV-radiation to enable Se(VI) and HCOOH adsorption to reach equilibrium. The temperatures for all the experiments were controlled at about 22 ± 2 °C.

2.3. Adsorption Data and Isotherm Determination of Se ions on TiO_2. Solutions containing sodium selenate with Se concentrations of 0.256 and 0.512 mM and HCOOH concentration ranging from 1 to 25 mMC were subjected to adsorption isotherm analysis. One liter of the solution was continuously purged with nitrogen for 30 min and adjusted to pH 3.5. TiO_2 powder (1.1 g) was then added, and the suspension was stirred continuously with magnetic stirrer for 30 min. After the suspension was filtered, the concentrations of Se and the total organic carbon in the filtrate were analyzed. The amount of Se or HCOOH adsorbed onto the TiO_2 particles was calculated from the difference between the initial and residual Se(VI) ions or HCOOH concentrations. All adsorption experiments were controlled at room temperature.

2.4. Analysis and Mathematical Modeling. All samples were taken using a syringe and then immediately filtered using a 0.22 μm low-protein-binding durapure (PVDF) membrane by Millipore. Total Se concentration (Se(VI)) in the filtrate was determined by a Varian induced coupled plasma-atomic emission spectroscopy instrument (ICP-AES). HCOOH concentration was determined by analyzing the total organic carbon (TOC) in the solution using a Shimadzu TOC-5000A analyzer. The Se(VI) photoreduction rates were estimated by zeroth-order rate law. The experimental data was then fitted in accordance to the proposed models by the mathematical software MicroMath Scientists by the least-squares methods.

Results and Discussion

3.1. Kinetic Modeling of Se(VI) Photocatalytic Reduction. In the current investigation, the pH was maintained at 3.5. At this pH, the TiO_2 surface is positively charged as the point of zero charge for Degussa P25 TiO_2 was found to be at pH 5.6. The positive charge on the TiO_2 surface at this pH was the result of protonation of the adsorbed water molecule and hydroxyl groups on the TiO_2 surface.[55−57] From our previous work,[53] it was found that below pH 2.5, very little of formic acid was adsorbed onto the catalyst surface due to its minimal ionization below this pH. An increase in pH led to increased HCOOH ionization ($pK_a = 3.77$)[58] and hence increased $HCOO^-$ adsorption onto the TiO_2 surface. Hence, at pH 3.5, the initial reactants, Se(VI) and HCOOH, exist as the negatively charged ions selenate (H_2SeO_4, $pK_a = -2.01 \pm 0.06$ and $HSeO_4^-$, $pK_a = 1.8 \pm 0.1$)[59,60] and $HCOO^-$ ions, respectively.

The presence of both the negatively charged Se(VI) and $HCOO^-$ ions in the solutions resulted in the competitive adsorption of these ions onto the positively charged TiO_2 surface. This was proven by equilibrium dark adsorption experiments of Se(VI) and HCOOH onto TiO_2 surface as shown in Figure 1. Se(VI) adsorption decreases with increasing concentration of HCOOH at constant initial Se(VI) concentration while higher Se(VI) initial concentration (Figure 1b) depressed formate adsorption. The former observation can be explained by the increased ionization of HCOOH as its concentration increased, hence a higher $HCOO^-$ adsorption onto the TiO_2 surface. This results in the competitive adsorption between the Se(VI) and $HCOO^-$ ions for the same site. The higher amount of Se(VI) adsorbed at the higher initial Se(VI) concentration of 0.512 mM would have resulted in less $HCOO^-$ being adsorbed

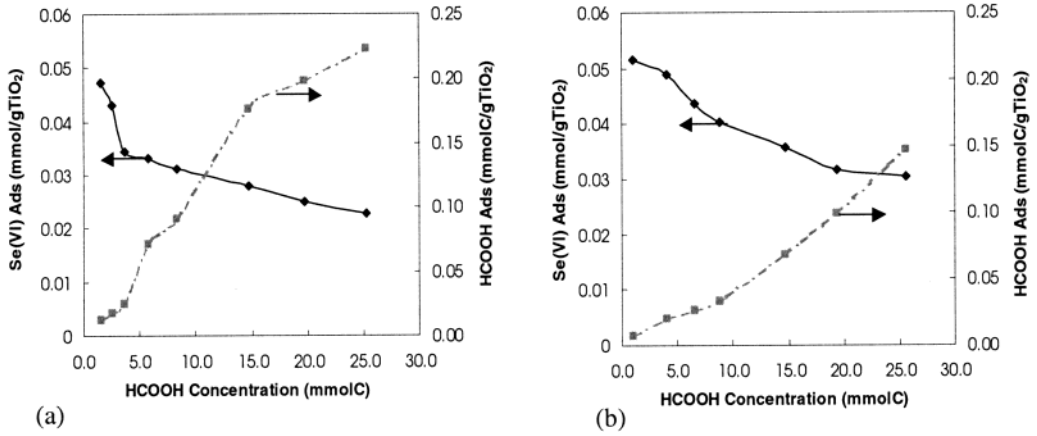

Figure 1. Equilibrium dark adsorption of Se(VI) and HCOOH on TiO_2 surface at (a) 0.254 mM (b) 0.512 mM initial Se(VI) concentrations, pH = 3.5, 293 K, 1 L of test solution, N_2 purging. (◆) Se(VI) adsorbed. (■) Formate adsorbed.

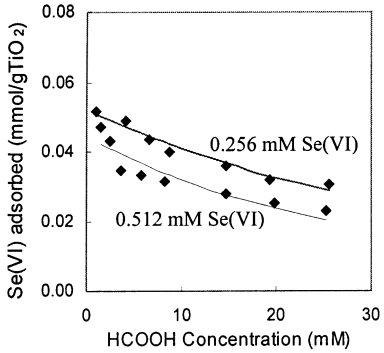

Figure 2. Comparison of experimental and modeled data for Se(VI) adsorption according to eq 1. $R^2 = 0.996$, $K_{Se} = 298$, $K_F = 0.079$. and $C_t = 0.071$.

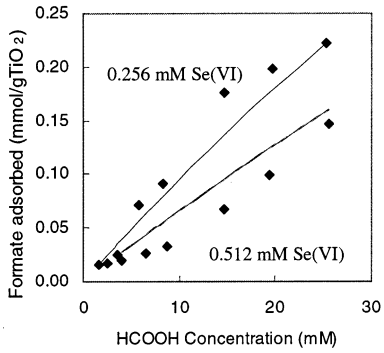

Figure 3. Comparison of experimental and modeled data for formate adsorption according to eq 2. $R^2 = 0.97$, $K_{Se} = 8.5 \times 10^5$, $K_F = 3.9$, and $C_t = 1.2$.

compared to that of 0.256 mM initial Se(VI) concentration, as manifested in Figure 1b.

Se(VI) adsorption in the presence of formate ions was modeled under the consideration that each Se(VI) ion possesses two negative charges, and hence, one Se(VI) ion is capable of being adsorbed onto two positively charged sites on the TiO_2 surface. A Se(VI) ion consists of four oxygen atoms bound to a central selenium atom, of which two of the oxygen atoms are negatively charged. The derivation of the Se(VI) Langmuir adsorption isotherm based on the above reasons gives the following equation (details of the derivation are included in the Appendix):

$$C_{Se_{ss}} = 0.5\left[\left(2C_t + \frac{(1+K_FC_F)^2}{K_{Se}C_{Se}}\right) \pm \sqrt{\left(4C_t + \frac{(1+K_FC_F)^2}{K_{Se}C_{Se}}\right)\left(\frac{(1+K_FC_F)^2}{K_{Se}C_{Se}}\right)}\right] \quad (1)$$

where C_{Sess} represents the Se(VI) ion adsorbed onto the two sites in the TiO_2 surface, K_{Se} and K_F are the adsorption constants for Se(VI) and $HCOO^-$, C_t represents the total available sites on the catalyst surface, and C_{Se} and C_F are the residual Se(VI) and formic acid concentrations at equilibrium, respectively.

Equation 1 indicates the possibility of 2 sets of solutions as shown by the "±" sign in the equation. The experimental data was successfully fitted when the equation with the "−" sign is used. A graphical representation of fitting the Se(VI) adsorption to eq 1 is presented in Figure 2 with the fitted parameters given in the figure captions. The fitting results show that eq 1 was able to describe the adsorption of Se(VI) in the presence of formate ions successfully. The fitted parameters were determined to have uncertainties of less than 5% of the regressed values. However, these parameters have no physical meaning and hence are not used to describe the surface processes.

Subsequently, formate adsorption in the presence of Se(VI) was derived. The derivation is given in the Appendix. This derivation assumes the adsorption of one formate ion onto one positively charged site on the TiO_2 surface in the presence of Se(VI) ions (assuming one Se(VI) ion is adsorbed onto two active sites):

$$C_{F_s} = \frac{K_FC_F}{2K_{Se}C_{Se}}[(-K_FC_F - 1) \pm \sqrt{(1+K_FC_F)^2 + 4C_tK_{Se}C_{Se}}] \quad (2)$$

where C_{Fs} represents the formate ion adsorbed onto one site on the TiO_2 surface. Other parameters have been previously defined.

Figure 3 shows the comparison of the experimental data with the modeled data from eq 3 when the equation with the "+" sign was used. The model provides a reasonable representation of the data. The average percentage difference between the experimental and calculated data is about 13.25%, showing a reasonable fit. The fitted parameters were determined to have uncertainties of about 10% of the regressed values. Similar to the discussion presented above, these parameters are only apparent and have no physical meaning.

To study the effect formic acid concentration on Se(VI) photoreduction, the Se(VI) photoreduction rates were plotted as a function of formic acid concentration and is shown in Figure 4. The insert in Figure 4 shows the concentration profile of

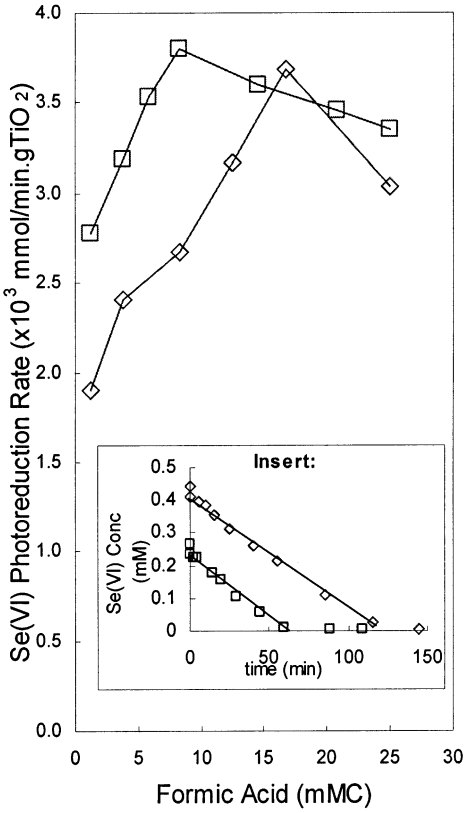

Figure 4. The effect of initial HCOOH concentration on the Se(VI) photoreduction rates. Insert: Se(VI) concentration profile versus time. Initial Se(VI) concentrations: (□) 0.256 mM, (◇) 0.512 mM. Experimental conditions: pH = 3.5, 1 L of test solution, 1.1 gTiO_2/L, N_2 purging, 293 K.

Se(VI) against time for two selected photoreduction experiments with initial Se(VI) concentrations of 0.256 and 0.512 mM, respectively. The drop in Se(VI) concentration at time = 0 min was attributed to Se(VI) dark adsorption onto TiO_2. After UV illumination, the decrease in Se(VI) concentration was attributed to the photoreduction of Se(VI) to Se, and can be described by the zeroth-order rate. For the range of Se(VI) concentrations in the present study, all other photoreduction rates were also found to obey the zero order rate with an average of R^2 value 0f 0.99.

Figure 4 shows the Se(VI) photoreduction rates obtained experimentally for HCOOH concentration ranging from 1 to 25 mMC and Se(VI) concentrations of 0.256 and 0.512 mM. The rates were optimum when the HCOOH concentrations were approximately 10 mMC and 15 mMC for initial Se(VI) of 0.256 and 0.512 mM, respectively. Higher HCOOH concentration suppressed the rates. The existence of an optimum formate ions concentration may be attributed to the optimum adsorption ratio of formate:Se(VI) ions, resulting in more efficient traps for both photogenerated electrons and holes. The existence optimum adsorption is also demonstrative that the redox reaction took place on the TiO_2 surface. The similar maximum photoreduction rate of about 3.7×10^{-3} mmol/min g TiO_2 obtained at the different initial Se(VI) concentrations, 0.256 and 0.512 mM, was also supportive of the occurrence of optimum conditions. Detailed discussion of the optimum adsorption ratio has been presented elsewhere.[53]

Assuming surface reaction being the rate-limiting step and the adsorption models represented by eqs 1 and 2 is reasonably accurate, the following expression was derived to describe the Se(VI) photoreduction rate using the Langmuir−Hinshelwood

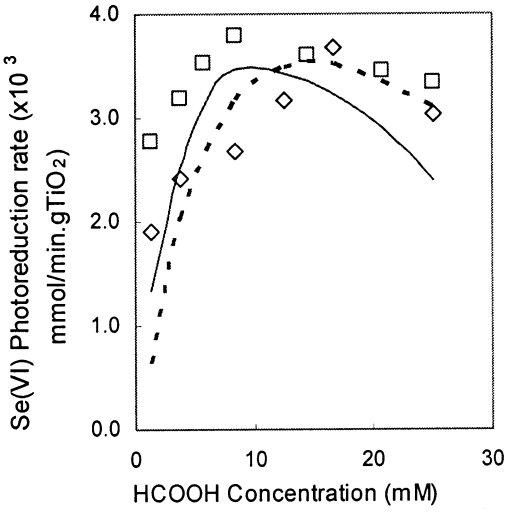

Figure 5. Comparison of experimental and modeled data for Se(VI) photoreduction rate according to eq 3. (□) Experimental rate. (—) Modeled rate for 0.256 mM initial Se(VI) concentration. (◇) Experimental rate. (- -) Modeled rate for 0.512 mM, initial Se(VI) concentration. $R^2 = 0.96$, $k_{rxn} = 4.77 \times 10^{-9}$, $K_{Se} = 1801.1$, $K_F = 64.3$, and $C_t = 1801.1$.

reaction mechanism:[61]

$$r' = k_{rxn} C_{Se_{ss}} C_{F_s}$$

$$= k_{rxn}\left\langle \frac{1}{2}\left\{\left[2C_t + \frac{(1+K_F C_F)^2}{K_{Se}C_{Se}}\right] - \sqrt{\left[4C_t + \frac{(1+K_F C_F)^2}{K_{Se}C_{Se}}\right]\left[\frac{(1+K_F C_F)^2}{K_{Se}C_{Se}}\right]}\right\}\right\rangle \left\{\frac{K_F C_F}{2K_{Se}C_{Se}}[(-K_F C_F - 1) + \sqrt{(1+K_F C_F)^2 + 4C_t K_{Se}C_{Se}}]\right\} \quad (3)$$

where r' is defined as the initial Se(VI) photoreduction rates and k_{rxn} is the apparent rate constant. Other parameters have been previously described.

Figure 5 shows the comparison of the experimental data with the modeled data for eq 3. It can be seen that the model fits the data reasonably well ($R^2 = 0.96$). The average percentage error between the experimental and calculated data from the model was determined to be about 15%. The optimum formic acid concentration reflected in the experimental data was also shown in the model. These fitted parameters only represent apparent constants with no physical meaning. The deviation of the newly derived rate model from the experimental rate may be explained as follows. The LH reaction mechanism assumes that the reactive sites are uniform and the surface reaction is the rate-determining step. The former assumption means that all active surface sites have the same attraction for the solute. However, the formation of Se particles due to photoreduction would have resulted in changes in the surface properties, hence affecting the dynamic adsorption of Se(VI) and formate ions onto the TiO_2 surface and resulting in the nonuniformity of the surface. When there are more Se deposits on the TiO_2 surface as the Se(VI) photoreduction proceeds, the desorption of Se might become rate-limiting. As observed from the experiments, Se did not desorb from the surface until H_2Se was evolved, which only happened after the Se(VI) was exhausted from the solution. The presence of Se deposits on the TiO_2 surface is most likely

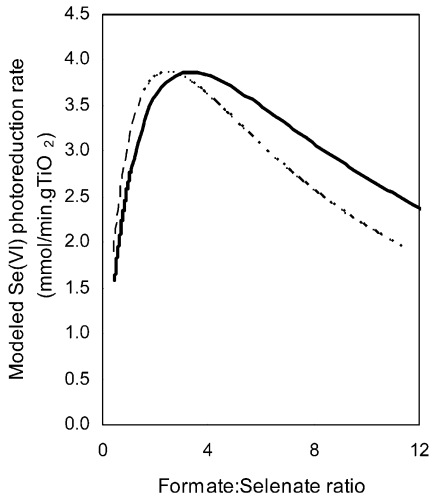

Figure 6. Optimization of eq 3 with respect to molar adsorption ratio of 3:1 at $HCOO^-$:Se(VI). (—) Modeled rate for 0.256 mM initial Se(VI) concentration. (- -) Modeled rate for 0.512 mM, initial Se(VI) concentration.

to block the reactive sites and hence affects the photoreduction rate. Another phenomenon unaccounted for in the above model was the change in the electrophoretic properties for illuminated TiO_2.[62,63] This would again affect the dynamic adsorption of the substrate onto the TiO_2 surface during illumination. The error in the adsorption models would inevitably contribute to the deviation as well.

The importance of the molar ratio of Se(VI) and $HCOO^-$ adsorbed onto the TiO_2 surface to give the maximum Se(VI) photoreduction rate has been highlighted in our previous investigations.[53] Maximum Se(VI) photoreduction rate was encountered when a molar adsorption of $HCOO^-$ and Se(VI) ions in the ratio of approximately 3:1 on the TiO_2 surface was achieved, which interestingly closely corresponded to stoichiometry of the redox reactions.[53] This experimental observation is also supported by the model (eq 3). Figure 6 shows the Se(VI) photoreduction rate as predicted by the new model as a function of the molar ratio of $HCOO^-$:Se(VI) ions adsorbed onto the TiO_2 surface. From the figure, it can be seen that the optimum photoreduction rate corresponded to the ratio of 3.3 ± 0.2 and 2.6 ± 0.1 for 0.256 and 0.512 mM initial Se(VI) concentration, respectively. These ratios are very close to the ratio of 3:1 suggested earlier.

As part of the kinetic studies, the effect of catalyst loading on the Se(VI) photoreduction rates was also investigated. The experiments were conducted with a catalyst loading ranging from 0.25 to 2.2 g TiO_2 L^{-1}. The results are shown in Figure 7. Increasing the catalyst loading increased the reduction rate constant until an optimum catalyst loading was attained at about 1.1 g/L. The enhanced reduction rate could be attributed to an increase in the availability of active sites as the number of particles increased. However, as particle concentration increased, the effect of interparticle interactions may cause light scattering and shadowing, hence reducing the amount of incident photons reaching the photosensitive TiO_2 surface,[64] leading to a decrease of photoadsorption efficiency. A greater extent of agglomeration could also arise from increased particle collision, hence resulting in decreased external active surface.[65]

Although the catalyst may not be explicitly regarded as a reactant, the nonlinear trend of the experimental data shown in

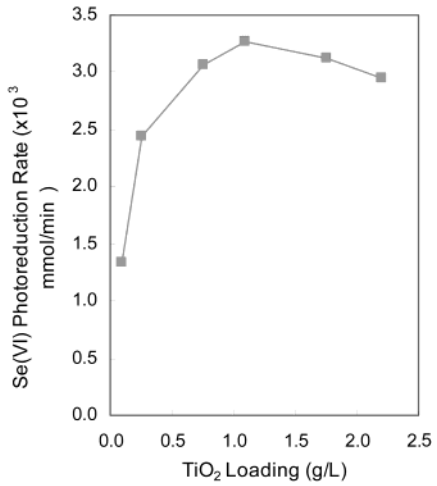

Figure 7. Influence of catalyst loading on Se(VI) photoreduction rate. Experimental conditions: pH = 3.5, 1 L of test solution, $[Se(VI)]_0 = 0.256$ mM, $[HCOOH]_0 = 16.7$ mMC, N_2 purging, 293 K.

Figure 7 may be fitted to the model below:[39,40]

$$r = \frac{k_c C_0}{\omega + C_0} \tag{4}$$

where k_c is the rate constant for the catalyst, C_0 is the catalyst concentration, ω is an attenuation factor accounting for light shielding, while the squared denominator indicated interparticle interactions.

The regression based on the eq 4 yielded an excellent agreement with a correlation coefficient of 0.99, while ω was evaluated as 0.93 g TiO_2 L^{-1} and k_c was 1.3×10^{-2} mol g TiO_2 L^{-2} min^{-1}.

From the use of all the information from the foregoing discussion, an empirical composite rate equation, which describes the competitive adsorption of the reactants and incorporating the effect of catalyst loading, may be derived as follows:

$$r' = k'_{rxn}\left\langle \frac{1}{2}\left\{\left[2C_t + \frac{(1+K_FC_F)^2}{K_{Se}C_{Se}}\right] - \sqrt{\left[4C_t + \frac{(1+K_FC_F)^2}{K_{Se}C_{Se}}\right]\left[\frac{(1+K_FC_F)^2}{K_{Se}C_{Se}}\right]}\right\}\right\rangle \left\{\frac{K_FC_F}{2K_{Se}C_{Se}}[(-K_FC_F - 1) + \sqrt{(1+K_FC_F)^2 + 4C_tK_{Se}C_{Se}}]\right\} \tag{5}$$

where

$$k'_{rxn} = \frac{k_{rxn}k_C C_0}{(\omega + C_0)^2}$$

where k_{rxn}' is the new reduction rate constant and it is a function of catalyst loading.

3.2. Proposed Mechanism. From the preceding investigation, it was found that the photocatalytic reduction of Se(VI) in the presence of HCOOH as the organic scavenger was strongly dependent on the adsorption of both Se(VI) and $HCOO^-$ ions. These ions adsorbed competitively on the same site. The following sequence of elementary reactions are proposed to explain the mechanism of photoreduction of Se(VI):

1. Complete dissociation of sodium selenate:

$$Na_2SeO_4 \rightarrow 2Na^+ + SeO_4^{2-} \quad (6)$$

2. Ionization of selenate and formic acid (pH and concentration dependent process). At pH 3.5, selenate ions exist as the unprotonated (SeO_4^{2-}) and formic acid is ionized to formate ions.

$$HSeO_4^- \rightarrow H^+ + SeO_4^{2-} \quad (7)$$

$$HCOOH \Leftrightarrow H^+ + HCOO^- \quad (8)$$

3. Competitive adsorption of ions onto hydrated TiO_2 sites (sites denoted by "*"):

$$SeO_4^{2-} + 2* \Leftrightarrow SeO_4^{2-(2*)} \quad (9)$$

$$HCCO^- \Leftrightarrow HCOO^-* \quad (10)$$

4. Photogeneration of electrons (e_{cb}^-) and holes (h_{vb}^+):

$$TiO_2 \xrightarrow{h\nu} e_{cb}^- + h_{vb}^+ \quad (11)$$

5a. Reduction of adsorbed Se(VI) ions by electrons:

$$SeO_4^{2-(2*)} + 8H^+ + 6e_{cb}^- \rightarrow Se^{0*} + 4H_2O \quad (12)$$

5b. Oxidation of adsorbed $HCOO^-$ ions by holes (or hydroxyl radicals):

$$HCOO^-* + 2h_{vb}^+ \rightarrow CO_2 + H^+ + * \quad (13)$$

6. Recombination of electrons and holes:

$$e_{cb}^- + h_{vb}^+ \rightarrow TiO_2 + \text{heat} \quad (14)$$

Balancing the electrons and holes generated in steps 5a and 5b (eq 12 and 13) results in 3 mol of $HCOO^-$ ions being oxidized when 1 mol of Se(VI) ions is reduced. This agrees with the arguments from our previous work that a molar adsorption of $HCOO^-$ and Se(VI) ions in the ratio of approximately 3:1 on the TiO_2 surface results in the optimum initial Se(VI) photoreduction rate. This is the result of efficient utilization of holes and electrons generated (for the oxidation of $HCOO^-$ and reduction of Se(VI), respectively), hence resulting in the efficient prevention of electron−hole recombination (step 6) at this ratio.[53]

4. Conclusion

New Se(VI) and formic acid adsorption models were derived assuming that one Se(VI) ion is adsorbed onto two active sites on the TiO_2 surface and the competitive adsorption of both Se(VI) and formate ions. The models fitted the experimental adsorption data reasonably well. The use of these adsorption models enabled the derivation of a rate equation on the basis of the LH reaction mechanism. The model confirmed that the optimum photoreduction rate of Se(VI) was achieved at formate-to-selenate molar adsorption ratios of 3.3 ± 0.2 and 2.6 ± 0.1 for 0.256 and 0.512 mM initial Se(VI) concentration, respectively, supporting the postulation for an optimum formate to selenate molar adsorption ratio of 3:1. A composite rate law incorporating the effect of catalyst loading was also derived. O the basis of the above model, a reaction mechanism describing the redox reaction based on the competitive adsorption of both Se(VI) and $HCOO^-$ ions and the subsequent scavenging of the photogenerated electrons and holes on the catalyst surface was proposed.

Acknowledgment. The author, Timothy Tan, acknowledges the Australian Institute of Nuclear Science and Engineering (AINSE) for financial support and The University of New South Wales and the Department of Education, Training and Youth Affairs (DETYA) for awarding the International Postgraduate Research Scholarship. The authors also thank Dr. Myint Zaw of the Environment Division, Australian Nuclear Science and Technology Organization (ANSTO), for his assistance in various aspects in the project.

Appendix

1. Derivation of Se(VI) and Formate Adsorption Model. The adsorption of Se(VI) (represented by Se) onto 2 adsorption sites (represented by S) to yield adsorbed Se(VI) ion (represented by Se_{SS}) is given as

$$Se + 2S \leftrightarrow Se_{SS}$$

Similarly, the adsorption of formate ion (represented by F) onto one adsorption site to yield adsorbed formate ion (represented by F_S) is given as

$$F + S \leftrightarrow F_S$$

If Se(VI) adsorption is assumed to be in equilibrium,

$$r_{AD-Se} = k_{Se}C_{Se}C_v^2 - k_{-Se}C_{Se_{SS}} = 0$$

where r_{AD-Se} represents the rate Se(VI) ions adsorbed onto the TiO_2 surface; k_{Se} and k_{-Se} are the forward and reversed adsorption rates, respectively; C_v represents the vacant sites available on the catalyst surface; and C_{Se} and C_F are the residual Se(VI) and formic acid concentrations at equilibrium, respectively.

For Se(VI) adsorption, the simplification of the above expression gives

$$\therefore C_{SeSS} = K_{Se}C_v^2C_{Se} \quad (I)$$

Similarly, for formate adsorption,

$$\therefore C_{FS} = K_FC_vC_F \quad (II)$$

If a site balance is performed,

$$C_t = C_v + C_{Se_{SS}} + C_{FS}$$

$$\therefore C_v = C_t - C_{Se_{SS}} - C_{FS} \quad (III)$$

where C_t represents the total sites available on the catalyst surface, C_v represents the vacant sites available on the catalyst surface, and C_{Sess} and C_{Fs} represent the site occupied by Se(VI) and formate ions, respectively.

A. To Derive Se(VI) Adsorption onto Two Sites in the Presence of Formate Ions. The substitution of eq III into eq II and making C_{Fs} the subject results in

$$\therefore C_{FS} = \frac{K_FC_F(C_t - C_{Se_{SS}})}{1 + K_FC_F} \quad (IV)$$

The substitution of eq IV and eq III into eq I results in

$$\frac{C_{Se_{ss}}}{K_{Se}C_{Se}} = \left[C_t - C_{Se_{ss}} - \frac{K_F C_F (C_t - C_{Se_{ss}})}{1 + K_F C_F}\right]^2 = \left(\frac{C_t - C_{Se_{ss}}}{1 + K_F C_F}\right)^2$$

$$\therefore \frac{(1 + K_F C_F)^2}{K_{Se}C_{Se}} C_{Se_{ss}} = C_t^2 - 2C_t C_{Se_{ss}} + {C_{Se_{ss}}}^2$$

$$\therefore {C_{Se_{ss}}}^2 - \left[2C_t + \frac{(1 + K_F C_F)^2}{K_{Se}C_{Se}}\right] C_{Se_{ss}} + C_t^2 = 0$$

For $ax^2 + bx + c = 0$

$$x = \frac{-b \pm \sqrt{b^2 - 4ac}}{2a}$$

$$\therefore C_{Se_{ss}} = \frac{\left[2C_t + \frac{(1 + K_F C_F)^2}{K_{Se}C_{Se}}\right] \pm \sqrt{\left[2C_t + \frac{(1 + K_F C_F)^2}{K_{Se}C_{Se}}\right]^2 - 4C_t^2}}{2}$$

The use of $a^2 - b^2 = (a + b)(a - b)$ for the expressions in the square root allows for the adsorption of Se(VI) onto two sites in the presence of formate ions to be derived as follows:

$$C_{Se_{ss}} = \frac{1}{2}\left\{\left[2C_t + \frac{(1 + K_F C_F)^2}{K_{Se}C_{Se}}\right] \pm \sqrt{\left[4C_t + \frac{(1 + K_F C_F)^2}{K_{Se}C_{Se}}\right]\left[\frac{(1 + K_F C_F)^2}{K_{Se}C_{Se}}\right]}\right\}$$

B. To Derive Formate Adsorption onto One Site in the Presence of Se(VI) Ions. The substitution of eq III into eq I results in

$$C_{Se_{ss}} = K_{se}C_{Se}(C_t - C_{se_{ss}} - C_{FS})^2$$

if $(a - b - c)^2 = a^2 + b^2 + c^2 - 2ab - 2ac + 2bc$ is used

$$\frac{C_{Se_{ss}}}{K_{se}C_{Se}} = {C_t}^2 + {C_{se_{ss}}}^2 + {C_{F_s}}^2 - 2C_t C_{se_{ss}} - 2C_t C_{F_s} + 2C_{se_{ss}} C_{F_s}$$

$$\therefore {C_{Se_{ss}}}^2 + \left(2C_{F_s} - 2C_t - \frac{1}{K_{Se}C_{Se}}\right) C_{Se_{ss}} + (C_t^2 - 2C_t C_{F_s} + {C_{F_s}}^2) = 0$$

$$\therefore {C_{Se_{ss}}}^2 + \left(2C_{F_s} - 2C_t - \frac{1}{K_{Se}C_{Se}}\right) C_{Se_{ss}} + (C_t - C_{F_s})^2 = 0$$

$$\therefore C_{Se_{ss}} = \frac{-\left(2C_{F_s} - 2C_t - \frac{1}{K_{Se}C_{Se}}\right) \pm \sqrt{\left(2C_{F_s} - 2C_t - \frac{1}{K_{Se}C_{Se}}\right)^2 - 4(C_t - C_{F_s})^2}}{2}$$

Again, the use of $a^2 - b^2 = (a + b)(a - b)$ for the expressions in the square root results in

$$\therefore C_{Se_{ss}} = \frac{-\left(2C_{F_s} - 2C_t - \frac{1}{K_{Se}C_{Se}}\right) \pm \sqrt{\left(-\frac{1}{K_{Se}C_{Se}}\right)\left(4C_{F_s} - 4C_t - \frac{1}{K_{Se}C_{Se}}\right)}}{2} \quad \text{(V)}$$

The substitution of eq V and eq III into eq II results in

$$C_{F_s} = K_F C_F \left(C_t - C_{F_s} + \frac{\left(2C_{F_s} - 2C_t - \frac{1}{K_{Se}C_{Se}}\right) \pm \sqrt{\left(-\frac{1}{K_{Se}C_{Se}}\right)\left(4C_{F_s} - 4C_t - \frac{1}{K_{Se}C_{Se}}\right)}}{2}\right)$$

$$\left[2\left(C_{F_s} + \frac{C_{F_s}}{K_F C_F} - C_t\right) - 2C_{F_s} + 2C_t + \frac{1}{K_{Se}C_{Se}}\right]^2 = \left(-\frac{1}{K_{Se}C_{Se}}\right)\left(4C_{F_s} - 4C_t - \frac{1}{K_{Se}C_{Se}}\right)\left(\frac{2C_{F_s}}{K_F C_F} + \frac{1}{K_{Se}C_{Se}}\right)^2 = -\frac{4C_{F_s}}{K_{Se}C_{Se}} + \frac{4C_t}{K_{Se}C_{Se}} + \frac{1}{(K_{Se}C_{Se})^2}$$

$$\frac{4}{(K_F C_F)^2} {C_{F_s}}^2 + \frac{4C_{F_s}}{K_F C_F K_{Se}C_{Se}} + \frac{4C_{F_s}}{K_{Se}C_{Se}} - \frac{4C_t}{K_{Se}C_{Se}} = 0$$

$$\frac{4}{(K_F C_F)^2} {C_{F_s}}^2 + \frac{(4 + 4K_F C_F)}{K_F C_F K_{Se}C_{Se}} C_{F_s} - \frac{4C_t}{K_{Se}C_{Se}} = 0$$

$${C_{F_s}}^2 + \frac{(K_F C_F + K_F^2 C_F^2)}{K_{Se}C_{Se}} C_{F_s} - \frac{(K_F C_F)^2 C_t}{K_{Se}C_{Se}} = 0$$

Similarly, for $ax^2 + bx + c = 0$,

$$x = \frac{-b \pm \sqrt{b^2 - 4ac}}{2a}$$

$$C_{F_s} = \frac{-\left[\frac{K_F C_F + (K_F C_F)^2}{K_{Se}C_{Se}}\right] \pm \sqrt{\left[\frac{K_F C_F + (K_F C_F)^2}{K_{Se}C_{Se}}\right]^2 + \frac{4C_t (K_F C_F)^2}{(K_{Se}C_{Se})^2} K_{Se}C_{Se}}}{2}$$

$$C_{F_s} = \frac{K_F C_F(-K_F C_F - 1) \pm \sqrt{[(1 + K_F C_F)^2 + 4C_t K_{Se}C_{Se}](K_F C_F)^2}}{2K_{Se}C_{Se}}$$

The adsorption of formate onto one site in the presence of Se(VI) ions is derived as follows

$$C_{F_s} = \frac{K_F C_F}{2K_{Se}C_{Se}}[(-K_F C_F - 1) \pm \sqrt{(1 + K_F C_F)^2 + 4C_t K_{Se}C_{Se}}]$$

References and Notes

(1) Oldfield, J. E. *Chemtech* **1995**, *March*, 52−55.
(2) Ike, M.; Takahashi, K.; Fujita, T.; Kashiwa, M.; Fujita, M. *Water Res.* **2000**, *34*, 3019−3025.

(3) Wang, D.; Alfthan, G.; Aro, A.; Makela, A.; Knuuttila, S.; Hammar, T. *Agric. Ecosyst. Environ.* **1995**, *54*, 137−148.
(4) Alaejos, M. S.; Romero, C. D. *Chem. Rev.* **1995**, *95*, 227−257.
(5) ATSDR Website: Agency for Toxic Substances and Disease Registry. http://www.atsdr.cdc.gov/toxprofiles/phs92.html.
(6) Ohlendorf, H. M.; Hoffman, D. J.; Saiki, M. K.; Aidrich, T. W. *Sci. Total Environ.* **1986**, *52*, 49−63.
(7) Sorg, T. J.; Logsdon, G. S. *J. Am. Water Works* **1978**, 379−393.
(8) Zhang, Y.; Moore, J. N. *Environ. Sci. Technol.* **1996**, *30*, 2613−2619.
(9) Masscheleyn, P. H.; Delaune, R. D; Patrick, H. P., Jr. *Environ. Sci. Technol.* **1990**, *24*, 91−96.
(10) Abdel-Moati, M. A. R. *Estuarine, Coastal Shelf Sci.* **1998**, *46*, 621−628.
(11) Kapoor, A.; Tanjore, T.; Viraraghavan, T. *Environ. Sci. Technol.* **1995**, *49*, 137−147.
(12) Boegal, J. V.; Clifford, D. A. EPA/600/2-86/031; EPA Publication: Cincinnati, OH, 1986.
(13) Gleason, K. J. Removal of Selenium from Contaminated Waters Using Emulsion Liquid Membranes. In *Chemical Separations with Liquid Membranes*; American Chemical Society: Washington, D.C., 1996; Chapter 24, pp 342−360.
(14) Kharaka, Y. K. *Appl. Geochem.* **1996**, *11*, 797−802.
(15) Murphy, A. *Ind. Eng. Chem. Res.* **1988**, *27*, 187−191.
(16) Myneni, S. C. B.; Tokunaga, T. K.; Brown, G. E., Jr. *Science* **1997**, *278*, 1106−1109.
(17) Refait, P.; Simon, L.; Genin, J. R. *Environ. Sci. Technol.* **2000**, *34*, 819−825.
(18) Qiu, S. R.; Lai, H. F.; Roberson, J.; Hunt, M. L.; Amrhein, C.; Giancarlo, L. C.; Flynn, G. W.; Yarmoff, J. A. *Langmuir* **2000**, *16*, 2230−2236.
(19) Fujita, M.; Lke, M.; Nishimoto, S.; Takahashi, K.; Kashiwa, M. *J. Ferment. Bioeng.* **1997**, *83*, 517−522.
(20) Garbisu, C.; Ishii, T.; Leighton, T.; Buchanan, B. B. *Chem. Geol.* **1996**, *132*, 199−204.
(21) Maiers, D. T.; Wichlacz, P. L.; Thompson, D. L.; Bruhn, D. F. *Appl. Environ. Microbiol.* **1988**, *54*, 2591−2593.
(22) Pelizzetti, E.; Minero, C.; Maurino, V. *Adv. Collioid Interface Sci.* **1990**, *32*, 271−316.
(23) Bems, B.; Jentoft, F. C.; Schlogl, R. *Appl. Catal.: Environ.* **1999**, *20*, 115−163.
(24) Fujishima, A.; Hashimoto, K.; Watanabe, T. New Tends in Photocatalyst Materials. In *TiO_2 Photocatalysis: Fundamentals and Applications*; Tryk, D. A., Ed.; BKC INC: Japan, 1999; Chapter 8, pp 124−131.
(25) Ku, Y.; Jung, I. L. *Water Res.* **2001**, *35*, 135−142.
(26) Kudo, A.; Domen, K.; Maruya, K.; Onishi, T. *Chem. Lett.* **1987**, 1019−1022.
(27) Kudo, A.; Domen, K.; Maruya, K.; Onishi, T. *J. Catal.* **1992**, *135*, 300−303.
(28) Navio, J. A.; Colon, G.; Trillas, M.; Peral, J.; Domenech, X.; Testa, J. J.; Padron, J.; Rodriguez, D.; Litter, M. I. *Appl. Catal. B: Environ.* **1998**, *16*, 187−196.
(29) Richard, C. *New J. Chem.* **1994**, *18*.
(30) Spacek, W.; Bauer, R.; Heisler, G. *Chemosphere* **1995**, *30*, 477−484.
(31) Surender, G. D.; Fotou, G. P.; Pratsinis, S. E. *Trends Chem. Eng.* **1998**, *4*, 145−159.
(32) Litter, M. I. *Appl. Catal. B: Environ.* **1999**, *23*, 89−114.
(33) Chen, D.; Ray, A. K. *Chem. Eng. Sci.* **2001**, *56*, 1561−1570.
(34) Tennakone, K.; Wijayantha, K. G. U. *J. Photochem. Photobiol. A: Chem.* **1998**, *113*, 89−92.
(35) Rophael, M. W.; Malati, M. A. *J. Chem. Soc. Commun.* **1987**, 1418−1420.
(36) Parent, Y.; Blake, D.; Magrini-Bair, K.; Lyons, C.; Turchi, G.; Watt, A.; Wolfrum, E.; Prairie, M. *Solar Energy* **1996**, *56*, 429−437.
(37) Vidal, A.; Diaz, A. I.; Hraiki, A. E.; Romero, M.; Muguruza, I.; Senhaji, F.; Gonzalez, J. *Catal. Today* **1999**, *54*, 283−290.
(38) Lewis, N. S.; Rosenbluth, M. L. Theory of Semiconductor Material. In *Photocatalysis: Fundamentals and Applications*; Serpone, N., Pelizzetti, E., Eds.; John Wiley & Sons: New York, 1989.
(39) Lea, J.; Adesina, A. A. *J. Photochem. Photobiol. A: Chem.* **1998**, *118*, 111−122.
(40) Bangun, J.; Adesina, A. A. *Appl. Catal. A: Gen.* **1998**, *175*, 221−235.
(41) Pareek, V. K.; Brungs, M. P.; Adesina, A. A. *Ind. Eng. Chem. Res.* **2001**, *40*, 5120−5125.
(42) Chen, D.; Ray, A. K. *Appl. Catal. B: Environ.* **1999**, *23*, 143−157.
(43) Matthews, R. W. *J. Catal.* **1988**, *111*, 264−272.
(44) Rideh, L.; Wehrer, A.; Ronze, D.; Zoulalian, A. *Catal. Today* **1999**, *48*, 357−362.
(45) Al-Ekabi, H.; Serpone, N. *J. Phys. Chem.* **1988**, *92*, 5726−5731.
(46) Chan, Y. C.; Chen, J. N.; Lu, M. C. *Chemosphere* **2001**, *45*, 29−35.
(47) Turchi, C. S.; Ollis, D. F. *J. Catal.* **1989**, *119*, 483−496.
(48) Gimenez, J.; Aguado, M. A.; Cervera-March, S. *J. Mol. Catal. A: Chem.* **1996**, *105*, 67−78.
(49) Alam, M.; Montalvo, R. A. *Metall. Mater. Trans. B* **1998**, *29B*, 95−140.
(50) Kikuchi, E.; Sakamoto, H. *J. Electrochem. Soc.* **2000**, *147*, 4589−4593.
(51) Sanuki, S.; Shako, K.; Nagaoka, S.; Majima, H. *Mater. Trans., JIM* **2000**, *41*, 799−805.
(52) Garcia, V. M.; Nair, P. K.; Nair, M. T. S. *J. Crystal Growth* **1999**, *203*, 113−124.
(53) Tan, T.; Beydoun, D.; Amal, R. *J. Mol. Catal.*, in press.
(54) Bruce, N. J. Chp 9: Actinometry. In *CRC Handbook of Organic Photochemistry*; Scarano, J. C., Ed.; CRC Press: Florida, 1989; Vol. 1, pp 241−259.
(55) Thurnauer, M. C.; Rajh, T.; Tiede, D. M. *Acta Chem. Scand.* **1997**, *51*, 610−618.
(56) Micic, O. I.; Zhang, Y.; Cromack, K. R.; Trifunac, A. D.; Thurnauer, M. C. *J. Phys. Chem.* **1993**, *97*, 7277−7283.
(57) Turchi, C. S.; Ollis, D. F. *J. Catal.* **1990**, *122*, 178−192.
(58) Chang, R. *Chemistry*, 5th ed.; McGraw-Hill: New York, 1994.
(59) Seby, F.; Potin-Gautier, M.; Giffaut, E.; Borge, G.; Donard, O. F. X. *Chem. Geol.* **2001**, *171*, 173−191.
(60) Linkson, P. B. *Trans. Ind. Chem. Eng.* **1992**, *70B*, 149−152.
(61) Fogler, H. S. *Elements of Chemical Rection Engineering*; Prentice Hall: New Jersey, 1992.
(62) Boxall, C.; Kelsall, G. H. . *Chem. Soc. Faraday Trans.* **1991**, *87*, 3357−3545.
(63) Boxall, C.; Kelsall, G. H. *J. Chem. Soc. Faraday Trans.* **1991**, *87*, 3347−3556.
(64) Herrmann, J. M. *Catal. Today* **1999**, *53*, 115−129.
(65) Wang, Z. H.; Zhuang, Q. X. *J. Photochem. Photobiol. A* **1993**, *75*, 105−111.